IEEE Journal of Translational Engineering in Health and Medicine

Received 9 December 2014; revised 13 May 2015; accepted 21 June 2015. Date of publication 29 June 2015; date of current version 21 July 2015.

Digital Object Identifier 10.1109/JTEHM.2015.2450735

A Comparison of Ultrasound Intima-Media Thickness Measurements of the Left and Right Common Carotid Artery

CHRISTOS P. LOIZOU[1], (Senior Member, IEEE), ANDREW NICOLAIDES[2], EFTHYVOULOS KYRIACOU[3], (Senior Member, IEEE), NIKI GEORGHIOU[2], MAURA GRIFFIN[2], AND CONSTANTINOS S. PATTICHIS[4], (Senior Member, IEEE)

[1]Department of Computer Science, Intercollege, Limassol 3507, Cyprus
[2]Cyprus Cardiovascular Disease Educational Research Trust, Nicosia 2368, Cyprus
[3]Department of Computer Science and Engineering, Frederick University, Limassol 3080, Cyprus
[4]Department of Computer Science, University of Cyprus, Nicosia 1678, Cyprus

CORRESPONDING AUTHOR: C. P. LOIZOU (panloicy@logosnet.cy.net)

ABSTRACT The intima-media thickness (IMT) of the common carotid artery (CCA) is an established indicator of cardiovascular disease (CVD). There have been reports about the difference between the left and the right sides of the CCA IMT and their relation with CVD. In this paper, we propose an automated system based on image normalization, speckle reduction filtering, and snakes segmentation, for segmenting the CCA, perform IMT measurements, and provide the differences between the left and the right sides. The study was performed on 1104 longitudinal-section ultrasound images acquired from 568 men and 536 women out of which 125 had cardiovascular symptoms (CVD). A cardiovascular expert manually delineated the IMT for the normal and the CVD groups. The corresponding (normal versus CVD) IMT mean $\pm$ standard deviation values for the left and the right sides were 0.74 ± 0.24 versus 0.87 ± 0.24 mm and 0.70 ± 0.17 versus 0.80 ± 0.18 mm, respectively. The main findings of this paper can be summarized as follows: 1) there was no significant difference between the CCA left side IMT and the right side IMT. These findings suggest that the measurement of the CCA IMT on one side only is needed for the normal group (and this is in agreement with other studies); 2) there were statistical significant differences for the IMT measurements between the normal group and the CVD group for both the left and the right sides; 3) there was an increasing linear relationship of the left and the right IMT measurements with age for the normal group; and to a lesser extend for the CVD group; 4) no statistical significant differences were found between the manual and the automated IMT measurements for both sides; and 5) the best result for classification disease modeling, using support vector machines, to discriminate between the normal and the CVD groups was a $64\% \pm 3.5\%$ correct classifications score when using both the left and the right IMT automated measurements. Further research is required for estimating differences and similarities between left and right intima media complex structure and morphology and their variability with texture features for differentiating between the normal and the CVD group.

INDEX TERMS B-mode, ultrasound imaging, common carotid artery, intima media thickness, IMT, cardiovascular disease.

I. INTRODUCTION

Cardiovascular disease (CVD) is the largest cause of death worldwide, though over the last two decades, cardiovascular mortality rates have declined in many high-income countries [1]. Atherosclerosis, which is a buildup on artery walls is the main reason leading to CVD and can result to heart attack, and stroke [1], [2]. Carotid intima-media-thickness (IMT) is a measurement of the thickness of the innermost two layers of the arterial wall and provides the distance between the lumen-intima and the media-adventitia

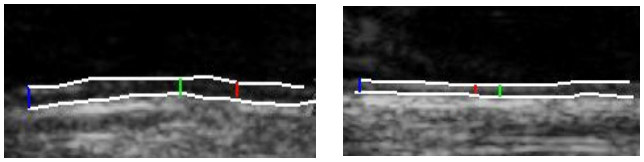

(a) (b)

FIGURE 1. Automated ultrasound imaging IMC segmentation of the CCA: a) left side (IMT_{mean} = 0.72 mm, IMT_{max} = 0.89 mm, IMT_{min} = 0.53 mm, IMT_{median} = 0.64 mm), and b) right side (IMT_{mean} = 0.56 mm, IMT_{max} = 0.61 mm, IMT_{min} = 0.39 mm, IMT_{median} = 0.55 mm), respectively. a) Left CCA IMC. (b) Right CCA IMC.

(see also Fig. 1). The IMT can be observed and measured as the double line pattern on both walls of the longitudinal images of the common carotid artery (CCA) [2] and it is well accepted as a validated surrogate marker for atherosclerosis disease. It is a fact that the increase in the IMT of the CCA is directly associated with an increased risk of myocardial infarction and stroke, especially in elderly adults without any history of CVD [1]–[3]. Noninvasive B-mode ultrasound imaging is used to estimate the IMT of the human carotid. Thus, the IMT may be used for the screening of population as at least half of premature heart attacks and strokes, can be prevented [1]–[3].

A plethora of studies were carried out measuring the ultrasound imaging common carotid IMT using both manual and automated techniques [4], [5]. Furthermore, a rather small number of studies investigated IMT measurements in both the left and right CCA as these are tabulated in Table 1 [6], [7]–[13]. IMT was measured in both CCA sides and expressed as the mean value obtained from these measurements [6], [9]. Yet it is not entirely clear whether the IMT is equal in both CCA arteries as several studies have shown a prediction for an increase of IMT in the left CCA. A theoretical, not well investigated, explanation has been raised, namely that increased shear stress forces in the left CCA contribute to this inequality [10], [11]. As it is well accepted that there are differences in shear stresses between the left and the right CCA, it can be supported that there are also differences in measurements as well as other mechanical characteristics between the two arteries. However, most studies presented in Table 1, were performed in adult individuals above the age of 50 years old [6]–[12], thus excluding the possibility to reveal the differences at an earlier stage of the disease [6]. It was also shown in [14], that the CCA IMT may be possibly used in the prediction of possible infarct side, and in the prediction of potential risk of stroke by evaluating the IMT on both sides of the CCA. There have been few studies regarding the effect of carotid IMT sidedness on the various risk factors associated with carotid IMT [9]–[11], [15]. Because of the different anatomical origins of the left versus the right CCA, it was speculated that hemodynamics, age, gender, blood lipid level, blood glucose level, and other risk factors would have different effects depending on whether the left or right CCA was considered [9]. In [10], the side differences in CCA IMT measurements, and their prognostic values, among patients with stable coronary artery disease, were evaluated. The study showed that the left and right CCA may exhibit different prognostic values in the investigated population.

The objective of this study was to investigate the intima media thickness measurement differences between the

TABLE 1. An overview of manual and automated IMT measurement studies for the left and right CCA in normal and cardiovascular disease groups.

Study	Year	Method	N	Left CCA mean(std) (mm)		Right CCA mean(std) (mm)		p-value	
				Manual	Auto	Manual	Auto	Manual	Auto
Normal Group									
Bots [11]	1997	Manual	1500	0.79(0.21)	-	0.78(0.22)	-	0.65	-
Schmidt [15]	1998	Manual/automated	50	0.88(0.25)	0.85(0.19)	0.86(0.24)	0.84(0.20)	0.43	0.49
Willekes [12]	1999	Manual/Ultramark	16	0.52(0.46)	0.49(0.45)	0.55 (0.42)	0.51(0.64)	0.55	0.83
Sun [8]	2002	Manual B-mode	1781	0.68(0.12)	-	0.66(0.12)	-	0.0004	-
Rodriquez [7]	2003	Manual B-mode	102	0.75(0.11)	-	0.71(0.11)	-	0.001	-
Arbel [6]	2007	-/M'ATH	98	-	0.625(0.078)	-	0.626(0.075)	-	0.884
Luo [9]	2011	QIMT	447	0.49(0.09)	-	0.47(0.09)	-	-	<u>0.002</u>
This study	2014	Manual/automated	976	0.74(0.20)	0.73(0.20)	0.70(0.17)	0.69(0.19)	0.56	0.77
CVD Group									
Bots [11]	1997	Manual	60	1.23(1.03)	-	1.29(1.08)	-	0.42	-
Willekes [12]	1999	Manual/Ultramark	13	0.74(0.74)	0.71(0.46)	0.73(0.61)	0.73(0.69)	0.67	<u>0.03</u>
Vicenzini [30]	2007	Manual	1655	-	0.97(0.21)	-	0.95(0.19)	-	<u>0.001</u>
Lee [10]	2011	Manual	149	0.83(0.24)	-	0.83(0.21)	-	0.72	-
This study	2014	Manual/automated	125	0.87(0.24)	0.86(0.23)	0.80(0.18)	0.81 (0.18)	0.02	<u>0.04</u>

CVD: Cardiovascular events; N: Number of cases investigated; significantly (shown underlined) and non-significantly different at $p<0.05$ and $p>=0.05$ respectively.

IEEE Journal of Translational Engineering in Health and Medicine

left and right CCA sides based on both manual and automated snake's based segmentation measurements. More specifically, the following questions will be addressed:

1) Is there a difference between CCA left side IMT and right side IMT for the normal group and the cardiovascular disease (CVD) group?
2) Is there a difference between left and right IMT measurements for the normal group versus the corresponding measurements for the cardiovascular disease group?
3) Is there an increase of left and right IMT measurements with age?
4) Can automated left and right IMT measurements be used to replace the manual measurements?
5) Can classification modelling be used to differentiate between the normal group, and the cardiovascular disease group based on left and right IMT measurements?

The findings may be helpful for the understanding of potential mechanisms that underlie the development of increase of carotid IMT at a relatively early stage of cardiovascular disease. The present study is an extension of the work in [16] where a significantly smaller number of subjects were analyzed (205 were analyzed in [16] versus 1104 that are analyzed in this study).

IMT can be measured through segmentation of the intima media complex (IMC), which corresponds to the intima and media layers (see Fig. 1) of the arterial wall. A number of techniques were proposed for the segmentation of the IMC in ultrasound images of the CCA which are discussed in [4] and [5]. In three recent studies performed by our group [17]–[19] we presented a semi-automatic method for IMC segmentation based on snakes, which was similar with the one used in this study. In [19] an automated system based on active contours and active contours without edges were proposed. The measurements were in all above cases [17]–[19] made on a normalized rectangular region of interest where speckle removal had been applied [20]. In [18], we presented an extension of the integrated system proposed in [17] where also the intima- and media-layers of the CCA could be segmented. The following section presents the materials and methods used in this study, whereas in section III, we present our results. Sections IV and V give the discussion, and the concluding remarks respectively.

II. MATERIALS & METHODS

A. RECORDING OF ULTRASOUND IMAGES

A total of 1104 B-mode longitudinal-section ultrasound images of the CCA which display the vascular wall as a regular pattern (see Fig. 1) that correlates with anatomical layers were recorded. The images were acquired from 568 men and 536 women at a mean $\pm$ std age of (59.27 ± 10.79) years, out of which 125 had cardiovascular symptoms (67.83 ± 8.92 years) and the rest 979 had no symptoms (58.18 ± 10.48 years). The ages of the two groups were statistically significantly different ($p=0.0001$).

The images were furthermore partitioned into three different age groups. In the first group, we included 224 images from patients who were younger than 50 years old (4 with CVD). In the second group, we had 400 patients who were 50–60 years old (25 with CVD). In the third group, we included 480 patients who were older than 60 years old (96 with CVD). A written informed consent was obtained according to the instructions of the local ethics committee.

The ATL HDI-5000 ultrasound scanner (Advanced Technology Laboratories, Seattle, USA) [21] was used with a linear probe (L12-5) covering the frequency range of 12 to 5 MHz. Assuming a nominal frequency of 7 MHz, sound velocity propagation of 1540 m/s and 2 cycles per pulse, we thus have a spatial pulse length of 0.44 mm (wavelength $\times$ number of cycles (0.22 mm $\times$ 2)) with an axial resolution of 0.22 mm (spatial pulse length) / 2) [21]. Images were captured at a resolution of 576 $\times$ 768 pixels with 256 grey levels. We used bicubic spline interpolation to resize all images to a standard pixel density of 16.66 pixels/mm (with a resulting pixel width of 0.06 mm) [17].

Brightness adjustments of ultrasound images were carried out in this study based on the method introduced in [23]. This improves image compatibility by reducing the variability introduced by different gain settings, different operators, different equipment, and facilitates ultrasound tissue comparability. Algebraic (linear) scaling of the images were manually performed by linearly adjusting the image so that the median gray level value of the blood was 0-5, and the median gray level of the adventitia (artery wall) was 180-190 [23]. The scale of the gray level of the images ranged from 0-255. Thus the brightness of all pixels in the image was readjusted according to the linear scale defined by selecting the two reference regions.

B. MANUAL IMT MEASUREMENTS AND SPECKLE REDUCTION FILTERING

A cardiovascular expert (with more than 40 years of clinical experience, co-author A.N. Nicolaides) manually delineated (using the mouse) the IMC [18] on all left and right longitudinal ultrasound images of the CCA after image normalization (see subsection II.A) and speckle reduction filtering (see end of subsection II.B). The IMC was measured by selecting 20 to 40 consecutive points for the intima and the adventitia layers. The manual delineations were performed using a system implemented in MATLAB (Math Works, Natick, MA) from our group. The measurements were performed between 1 and 2 cm proximal to the bifurcation of the CCA on the far wall over a distance of 1.5 cm starting at a point 0.5 cm and ending at a point 2.0 cm proximal to the carotid bifurcation. The bifurcation of the CCA was used as a guide, and all measurements were made from that region. The IMT was then calculated as the average of all the measurements. The measuring points and delineations were saved for comparison with the snake's segmentation method. All sets of manual segmentation measurements were performed by the expert in a blinded manner, both with

respect to identifying the subject and delineating the image. The correctness of the work carried out by a single expert was monitored and verified by at least another expert.

For speckle reduction, the filter DsFlsmv (despeckle filter linear scaling mean variance-DsFlsmv, first introduced in [24], and evaluated for ultrasound images of the carotid in [20], was applied prior to IMC segmentation. The filters of this type utilize first order statistics such as the variance and the mean of a pixel neighborhood and may be described with a multiplicative noise model [25]. The moving window size for the despeckle filter DsFlsmv was 5×5 and the number of iterations applied to each image was two.

C. SNAKES SEGMENTATION

Before running the IMC snakes segmentation algorithm, an IMC initialization procedure was carried out for positioning the initial snake contour as close as possible to the area of interest [17]. The Williams & Shah snake segmentation method [26] was used to deform the snake and segment the IMC borders in each image. The snake contour, $v(s)$, adapts itself by a dynamic process that minimizes an energy function ($E_{snake}(v, s)$) defined as [26]:

$$\begin{aligned} E_{snake}(v(s)) &= E_{\text{int}}(v(s)) + E_{image}(v(s)) + E_{external}(v(s)) \\ &= \int_s (\alpha_s E_{cont}(v(s)) + \beta_s E_{curv}(v(s)) \\ &\quad + \gamma_s E_{image}(v(s)) + E_{external}(v(s)))ds. \end{aligned} \quad (1)$$

where $E_{\text{int}}(v(s))$, $E_{image}(v(s))$, $E_{external}(v(s))$, $E_{cont}(v(s))$, $E_{curv}(v(s))$ are the internal, image, external, continuity, and curvature energies of the snake, and $\alpha(s)$, $\beta(s)$ and, $\gamma(s)$ the strength, tension and stiffness parameters respectively. The method was proposed and evaluated in [17], in 100 ultrasound images of the CCA and more details about the model can be found there. For the Williams & Shah snake, the strength, tension and stiffness parameters were equal to $\alpha_s = 0.6$, $\beta_s = 0.4$, and $\gamma_s = 2$ respectively. The extracted final snake contours (see Fig. 1), corresponds to the adventitia and intima borders of the IMC. The distance is computed between the two boundaries, at all points along the arterial wall segment of interest moving perpendicularly between pixel pairs, and then averaged to obtain the mean IMT (IMT_{mean}). Also the maximum (IMT_{max}), minimum (IMT_{min}), and median ($\text{IMT}_{\text{median}}$) IMT values, were calculated.

D. CARDIOVASCULAR DISEASE CLASSIFICATION MODELLING

Cardiovascular disease classification modelling was used to differentiate between the normal and the CVD group based on the left and right IMT measurements and age. The C-support vector classification (C-SVM) network [27] was investigated using the Gaussian Radial Basis Function (RBF) kernel and the linear kernel. Significantly better performance was obtained using the RBF kernel tuned based on the methodology proposed in [27] using a grid-search approach for the values of c and γ. More specifically, runs were performed on randomly selected groups of 100 normal and 100 CVD subjects above the age of 50 years old. For each set of features the procedure was repeated for 10 times and the average results were computed. The leave-one-out method was used for validating all the classification models. The performance of the classifier models was measured using the receiver operating characteristic (ROC) metrics: true positives (TP), false positives (FP), false negatives (FN), true negatives (TN), sensitivity (SE), specificity (SP) and the area under the ROC curve (AUC). We also computed the percentage of correct classifications score (%CC) based on the correctly and incorrectly classified cases.

E. STATISTICAL ANALYSIS

The Wilcoxon rank sum test was used in order to identify if for each set of IMT measurements a significant difference (S) or not (NS) exists between the extracted IMT measurements, with a confidence level of 95%. The Mann-Whitney rank-sum test was also used in order to identify significant differences between the different groups. For significant differences, we require $p<0.05$. Furthermore, box plots for the two different structures, were plotted for the left and right CCA. Bland–Altman plots [13], with 95% confidence intervals, were also used to further evaluate the agreement between the left and right IMT measurements. Also, the Pearson correlation coefficient, ρ, between the left and right automated IMT measurements, as well as the manual and automated IMT measurements were investigated, which reflects the extent of a linear relationship between two data sets. Furthermore, we used regression analysis to investigate the relationship between the IMT left and right CCA measurements and age.

III. RESULTS

Figure 1a) illustrates an example of the automated IMC segmentations of the left side CCA ($\text{IMT}_{\text{mean}} = 0.72$ mm, $\text{IMT}_{\text{max}} = 0.89$ mm, $\text{IMT}_{\text{min}} = 0.53$ mm, $\text{IMT}_{\text{median}} = 0.64$ mm), while Fig. 1b) shows the right side CCA ($\text{IMT}_{\text{mean}} = 0.56$ mm, $\text{IMT}_{\text{max}} = 0.61$ mm, $\text{IMT}_{\text{min}} = 0.39$ mm, $\text{IMT}_{\text{median}} = 0.55$ mm) respectively. The image was acquired from an asymptomatic male subject at the age of 52. It is shown, for this example that left and right IMT measurements of the CCA are different.

Table 2 presents the manual and automated mean, standard deviation, median, minimum and maximum measurements for the left and right CCA IMT for the normal (N=976) and cardiovascular disease (N=125) subjects. It is shown that the left CCA IMT side has slightly higher measurements than the right side for both the manual and automated measurements for both the normal and CVD subjects. However, there were no significant differences between the left and the right side IMT measurements for the normal group, but there were significant differences between the two sides for the CVD group. We also found higher IMT mean and median values for the subjects that already developed CVD events when compared to the normal group.

IEEE Journal of Translational Engineering in Health and Medicine

TABLE 2. Manual and automated mean, standard deviation, median, minimum and maximum values for the left and right CCA ultrasound imaging IMT in normal and cardiovascular disease subjects.

	Left CCA					Right CCA					
	Mean	Std	Median ^{1}Q1/Q2/Q3	Minimum ^{1}Q1/Q2/Q3	Maximum ^{1}Q1/Q2/Q3	Mean	Std	Median ^{1}Q1/Q2/Q3	Minimum ^{1}Q1/Q2/Q3	Maximum ^{1}Q1/Q2/Q3	p-values
Normal Subjects (N=976)											
IMT_{man}	0.74	0.2	0.61/**0.71**/0.81	0.31/**0.51**/0.64	0.66/**0.75**/0.89	0.7	0.2	0.60/**0.70**/0.80	0.20/**0.47**/0.62	0.59/**0.70**/0.91	0.67/0.56/0.34/0.78
IMT_{auto}	0.73	0.2	0.62/**0.73**/0.84	0.23/**0.48**/0.63	0.68/**0.78**/0.90	0.69	0.2	0.60/**0.72**/0.81	0.23/**0.48**/0.60	0.63/**0.73**/0.88	0.46/0.77/0.72/0.85
Cardiovascular Disease (CVD) Subjects (N=125)											
IMT_{man}	0.87	0.2	0.71/**0.81**/1.01	0.39/**0.53**/0.71	0.71/**0.85**/1.05	0.8	0.2	0.71/**0.81**/0.91	0.33/**0.52**/0.66	0.66/**0.82**/0.98	0.03/0.04/0.01/0.03
IMT_{auto}	0.86	0.2	0.70/**0.82**/1.06	0.31/**0.53**/0.71	0.72/**0.89**/1.09	0.81	0.2	0.69/**0.80**/0.89	0.36/**0.53**/0.66	0.67/**0.81**/0.99	0.04/0.02/0.02/0.03

IMT_{man}, IMT_{auto},: Manual and automated Left and Right IMT measurements. ^{1}Q1, Q2, Q3: Quartile values corresponding to P25%, P50% and P75% respectively given for minimum, median and maximum respectively. Median values are given in bold. The p-values in the last column refer to Wilcoxon rank sum test performed on the Left vs Right sides at $p<0.05$ for the mean, median, minimum and maximum IMT measurements. Underlined values show significant difference.

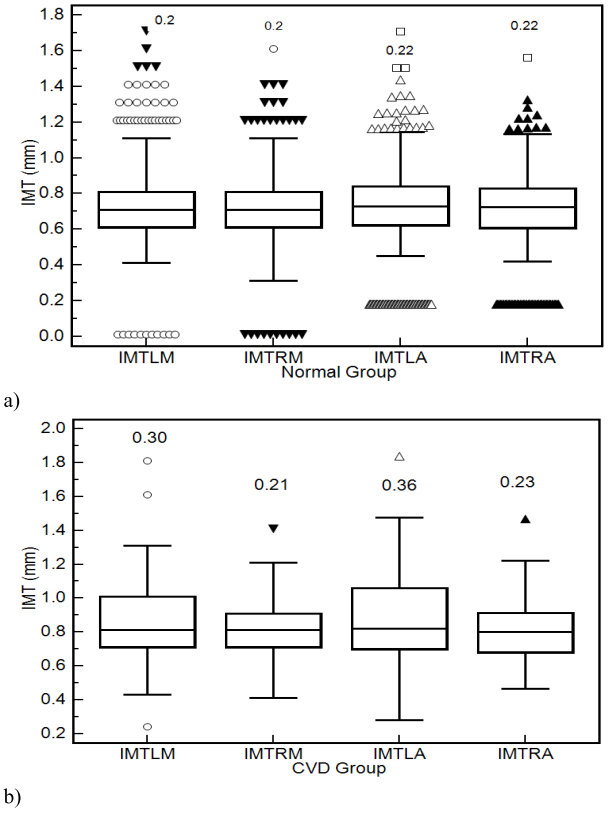

FIGURE 2. Box plots for the left and right CCA IMT manual measurements (IMTLM, IMTRM) and automated measurements (IMTLA, IMTRA) for a) normal and b) CVD groups respectively. Inter-Quartile Range (IQR) values are shown above the box plots. Straight lines connect the nearest observations with 1.5 of the IQR of the lower and upper quartiles. Unfilled circles, inverted filled triangles, unfilled triangles and filled triangles correspond to outliers with values beyond the ends of the 1.5xIQR; whereas filled inverted triangles, unfilled circles and unfilled squares correspond to outliers within 2.5XIQR and 3.5xIQR respectively.

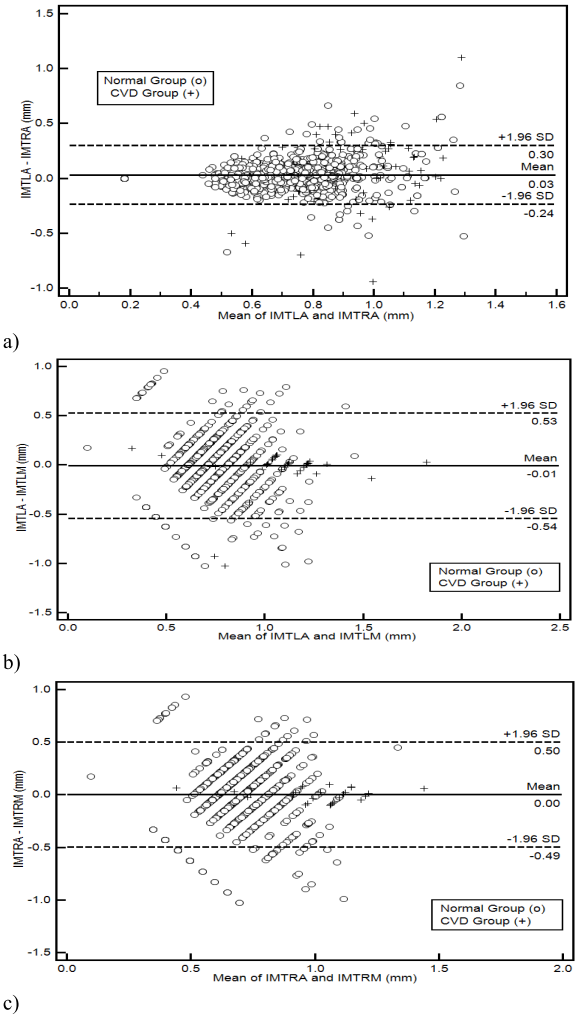

FIGURE 3. Regression lines (Bland–Altman plots) of a) automated IMT left and right measurements, b) IMT left automated versus manual and c) IMT right automated versus manual. Normal subjects are indicated with circles while CVD subjects are indicated with crosses.

Figure 2 illustrates box plots for the left and right sides CCA IMT manual measurements (IMTLM, IMTRM) and automated measurements (IMTLA, IMTRA) for the normal (see Fig. 2a) and b) CVD subjects (see Fig. 2b) respectively. No significant differences were found between the manual and the automated IMT measurements for both the normal and the CVD groups (using the Wilcoxon rank-sum test: 1. Normal group: Left CCA p=0.72, Right CCA p=0.67, 2. CVD group: Left CCA p=0.92, Right CCA p=0.64).

Figure 3a) illustrates a Bland–Altman plot between the left and the right automated segmentation measurements of the IMT. The difference of the two measurements between left and right IMT sides was (0.03+0.27) mm and (0.03-0.20) mm. In Fig 3b) we show the Bland-Altman plot between the left manual versus automated

TABLE 3. Median IMT left and right, manual and automated segmentation comparisons based on the Wilcoxon rank sum test at p<0.05 and the correlation coefficient, ρ, for normal (n=976) and cardiovascular groups (CVD) (n=125). also comparisons for three different age groups, <50 (n=228), 50-60 (n=393), >60 (n=480) are given.

	Left vs Right CCA		Left CCA	Right CCA
	Normal	CVD	Normal vs CVD	Normal vs CVD
Manual	NS (0.56) ρ=0.59 (p=0.001)	S (0.04) ρ=0.37 (p=0.0001)	S (0.004) ρ=0.11 (p=0.006)	S(0.045) ρ=0.33 (p=0.001)
	S (0.0001)/S(0.001)/S(0.001) ρ=0.37/ρ=0.72/ρ=0.67	NS(0.7)/S(0.03)/NS(0.08) ρ=0.45/ρ=0.56/ρ=0.78	NS(0.23)/S(0.001)/S(0.001) ρ=0.61/ρ=0.33/ρ=0.29	NS(0.43)/S(0.001)/S(0.001) ρ=0.45/ρ=0.77/ρ=0.82
Automated	NS (0.77) ρ=0.84 (p=0.0014)	S (0.02) ρ=0.47 (p=0.001)	S (0.02) ρ=0.83 (p=0.01)	S(0.023) ρ=0.84 (p=0.001)
	S(0.02)/S(0.01)/S(0.02) ρ=0.31/ρ=0.53/ρ=0.45	NS(0.7)/S(0.02)/S(0.03) ρ=0.49/ρ=0.64/ρ=0.78	NS(0.55)/S(0.04)/S(0.001) ρ=0.66/ρ=0.42/ρ=0.59	NS(0.39)/S(0.031)/S(0.051) ρ=0.49/ρ=0.65 /ρ=0.91

p-values are given in parentheses. S, NS indicates significant and Non-significant difference at p≤0.05. Underlined values show significant difference.

IMT measurements with a difference between manual and automated measurements of (−0.02+0.56) mm and (−0.02-0.60) mm. Figure 3c) illustrates the Bland-Altman plot between the right automated versus manual IMT measurements with a difference between manual and automated measurements of (−0.01+0.53) mm and (−0.01-0.55) mm respectively.

The left side of Table 3 presents the results after performing the non-parametric Wilcoxon rank sum test, at p<0.05, between the left and the right CCA, for both the manual and automated measurements. The right side of Table 3 shows the comparisons made for the left and right CCA for the normal group versus the CVD group. No significant differences were found for the normal group while significant differences were found for the CVD group between the left and the right CCA IMT measurements (as documented in Table 2). The Mann-Whitney rank-sum test performed between the manual and the automated IMC segmentation measurements for three different age groups (<50, 50-60, >60) showed that significant differences exist for both the left and the right sides when comparing the normal group versus the CVD group for the age groups 50-60 and above 60 years of age.

Figure 4a) and Fig. 4b), illustrate the results of the mean left automated (IMTLA) versus the mean right automated (IMTRA) IMT measurements using regression analysis for the normal and the CVD group respectively. In Fig. 4a) we have an intercept of 0.0983 and a slope of 0.904 with a standard error of 0.0144 and 0.0197 of the intercept and the slope respectively and an F-ratio of 2849.16. The correlation coefficient was 0.88 (p=0.11). It is shown that the IMT exhibits a linear relationship between the two sides. Figure 4a) also shows that the confidence interval limits for the IMT for the left and right sides are ±0.21 mm. In Fig. 4b) we have an intercept of 0.476 and a slope of 0.481 with a standard error of 0.08985 and 0.1085 of the intercept and a slope respectively and an F-ratio of 2333.76. The correlation coefficient was 0.73 (p=0.07). Furthermore, it is shown that in this study the values of the IMT in a normal carotid artery may vary between 0.20 and 0.91 mm, while the values for the

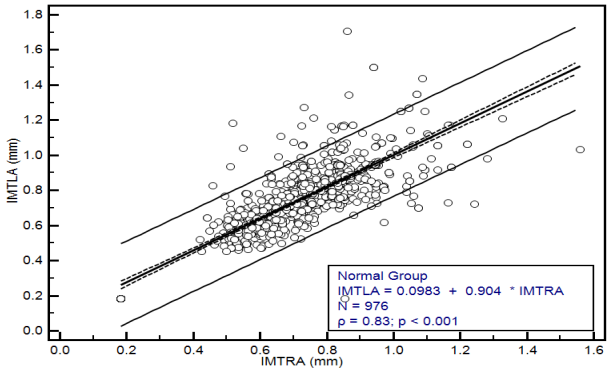

a)

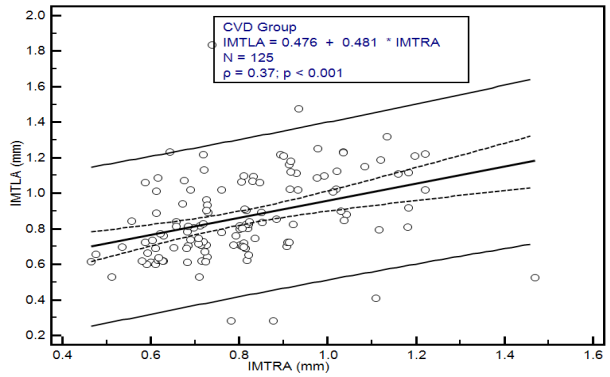

b)

FIGURE 4. Regression lines for the automated IMTLA versus IMTRA in (mm) with confidence interval limits of ±0.21 and confidenece intervals for the correlation coeficient (dashed) for a) the Normal Group, and b) the CVD Group of all subjects investigated in this study.

CVD group may very between 0.21 and 1.05 mm (see also Table 2), depending on age, and this is also consistent with other studies [4]–[14], [29].

Figure 5a presents regression plots showing a linear increase of the left automated CCA IMT with age for the normal group with a correlation coefficient $\rho = 0.1$ (p=0.001) whereas Fig. 5b illustrates a linear increase of the left automated CCA IMT with age for the CVD group with a correlation coefficient $\rho = 0.16$ (p=0.075).

IEEE Journal of Translational Engineering in Health and Medicine

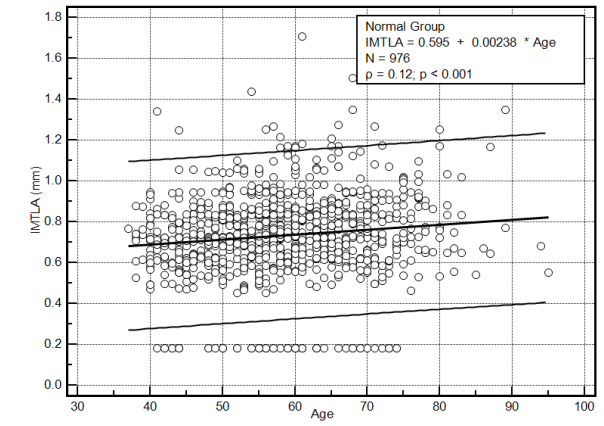

a)

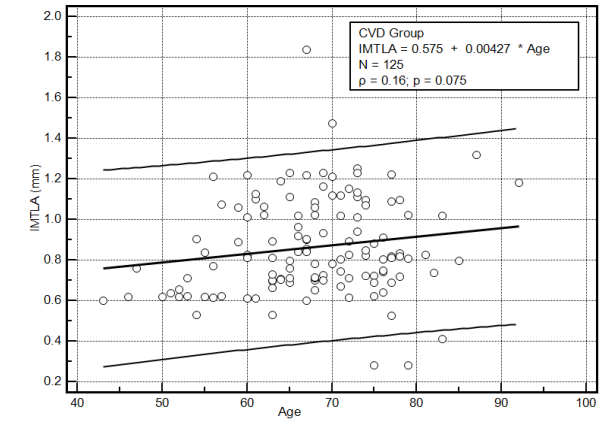

b)

FIGURE 5. **Regression plots showing in a) the linear increase of the left automated CCA IMT with age for the Normal Group with a correlation coefficient $\rho = 0.12$ (p=0.001) and b) the linear increase of the left automated CCA IMT with age for the CVD Group with a correlation coefficient $\rho = 0.16$ (p=0.075). (ρ given in the box corresponds to the correlation coefficient and p corresponds to the significance level).**

TABLE 4. **Normal vs cardiovascular disease classification models based on the IMT manual (M) and automated (A) measurements using SVM with RBF kernels.**

IMT			Classification Models Results			
Left	Right	M/A	CC %	Sensitivity%	Specificity%	AUC
x		M	59±4.6	75±8.5	43±9.0	0.575±0.0412
x		A	58±4.2	80±8.8	37±4.9	0.617±0.0408
	x	M	58±3.6	73±9.9	44±9.1	0.562±0.0301
	x	A	56±3.1	54±16.5	58±18.5	0.593±0.0402
x	x	M	59±5.0	74±6.3	44±6.8	0.587±0.0411
x	x	A	**64±3.5**	77±9.2	51±5.2	**0.655±0.0306**

Table 4 tabulates the results of the cardiovascular disease classification modelling for classifying a subject as normal or CVD. It is shown that the best results were obtained with the combination of both the left and the right automated IMT measurements with a correct classifications score of 64 $\pm$ 3.5%. The corresponding model for the manual measurements gave a correct classifications score of 59 $\pm$ 5.0%. Models derived with the manual left or right gave very similar performance to the model when both measurements were combined.

IV. DISCUSSION

The results of this study showed that:

1) There is a difference between the CCA left side IMT and the right side IMT. The left side IMT is slightly higher than the right side IMT (see Table 2 and Table 3). However, there was no significant difference between the left side and right side IMT measurements for the normal group. Similar findings to these were also reported in [11] by Bots *et al.*, where they have investigated 1500 cases, in [15] by Schmidt and Wendelhag, where they have investigated 50 cases, and in [12] in 16 cases (as documented also in Table 1). Moreover, the IMT measurements of this study are very close to the studies in [7] and [12] as tabulated in Table 1. There were only two studies [7], and [8] that showed significant differences between the left and the right sides for the normal group. Significant differences between the left and the right sides were shown for the CVD group for this study as well as in [12] and [30]; in contrast to the findings of the study in [10] that showed no significant differences between the two sides (see Table 1).
2) We found significant differences between the normal group and the CVD group for both the left and the right sides IMT measurements (see Table 3). In addition there were significant differences between the normal group and the CVD group for the age groups 50-60, and >60 years old. These findings are also in agreement with [9]. Moreover, as expected, subjects from the CVD group exhibit higher IMT measurements when compared to the normal group. This finding is also in agreement with the study of [10].
3) We have also found an increasing linear relationship of the left and right IMT measurements with age for the normal group as also found in other studies [9], [16], [30], [31] (see Fig. 5a). A low linear relationship was also estimated for the CVD group (see Fig. 5b). We have furthermore shown that there is a linear relationship between the left and the right sides IMT measurements (see Fig. 4) for both the normal and the CVD groups and for both the manual and the automated segmentation measurements. These findings are in agreement with other studies [31]–[35]. It should be furthermore noted that the low correlation coefficients found in Fig. 4b) and Fig. 5 are due to the scattering of the IMT measurements especially for the CVD group.
4) No statistical significant differences were found between the automated and the manual IMT measurements for both CCA sides and therefore automated measurements may be used to replace the manual measurements. No significant differences between the automated and the manual IMT measurements were also reported in [6], [10]–[12], and [15]. The mean difference between the manual and the automated mean IMT measurements found in this study was 0.01 mm, which is in the same order as also found in other studies

performed by our group [17], [18], [36], [37] and also documented in [4].

5) Classification disease modelling should be used with caution to differentiate between the normal group and the cardiovascular disease group based on either the left or the right or both IMT measurements. The highest correct classifications score achieved was 64 ± 3.5% using the automated left and right IMT measurements. These results merit further investigation how to improve their performance further.

A number of studies were performed, either on normal or on CVD subjects, for investigating the differences between the left and right CCA sides (see also Table 1). More specifically, in [6], 98 healthy adults with a mean age of 28 years underwent blood tests to evaluate various CVD risk factors as well as automated ultrasonic measurements of their CCA IMT on both carotid arteries. No significant difference was noted between the IMT on both sides as also reported in the present study. That was probably due to the fact that the sample investigated was from young healthy individuals. The IMT on the left CCA artery in 52 men was 0.625 ± 0.078 mm while on the right CCA it was 0.626 ± 0.075 mm (p=0.884). The IMT values in 46 women were 0.615±0.059 mm while on the right it was 0.622±0.0618 mm (p=0.582), respectively. As reported in the literature differences between the left and right CCA occur in older people due to a combined effect of various atherosclerotic risk factors as well as due to the potential differences between the shear forces between the two carotid arteries [6]. In other studies [7], [8], as well as in the present study an increase of IMT on the left CCA in older individuals was found. This was not the case in [6], where a group of young and healthy adults were investigated. It is possible that if mechanical stress forces contribute to an enhanced left IMT, it takes a relatively long time to become evident. In [9], 447 healthy people were assigned into six age groups and their left and right IMT as well as other hemodynamic parameters were measured. It was shown that the left CCA IMT was thicker than the right between the ages of 35 and 65 years old. It was furthermore shown that the left CCA IMT showed no obvious change before the age of 35 years, and after the age of 35 the CCA IMT thickened considerably every 10 years. Such a trend in the right CCA IMT was noted to occur 10 years later, i.e., it did not change significantly before the age of 45 years and IMT thickening occurred only after the age of 45. It was finally concluded that hemodynamic and biochemical changes had different effects on the IMT depending on the side affected. In another study [15], manual measurements of the left and right CCA IMT were performed on 50 healthy individuals. It was shown that the inter-observer variability in IMT measurements was smaller when images were recorded from both the right and the left CCA sides than the images recorded from only the right CCA. Willekes *et al*. [12], evaluated the IMT for both left and right CCA on 16 young normal and 13 old CVD subjects. It was shown that older subjects exhibited a larger IMT when compared to the younger subjects. No statistical significant differences were found between left and right CCA sides.

In [11], associations between the CCA IMT and prevalent CVD and presence of lower extremity arterial atherosclerosis were found both in the left and the right CCA sides. It was concluded that the average of both near and far wall measurements of the CCA provides a good indicator of CVD disease.

In [29] the relation of carotid IMT and the presence of vascular risk factors and correlates of the IMT with the degree of the distal internal carotid stenosis and the proximal CCA resistive index were investigated in 1655 patients. Significant side differences were found with higher IMT on the left side (left CCA, 0.97 ± 0.21 mm with $p<0.001$, right CCA, 0.95±0.19 mm with $p<0.001$. The results in [38], confirmed the relation of vascular risk factors with age being the most relevant. Additionally increased wall shear stress was noted in the left side of the CCA.

In [10], correlations between the left and right CCA side were investigated in 149 patients with coronary artery disease. No significant differences were found for the IMT between the left and right CCA sides. The authors concluded that the non-significant differences found between the two CCA sides, may be due to the fact that a small number of samples was selected as well as to the population selected. It was also shown that the left and right CCA IMT exhibited different predictive values on CVD events, suggesting differential correlations between the two different sides with CVD risk factors and clinical outcomes.

Given the different anatomy of each CCA side, it was proposed in the literature, but not thoroughly investigated, that the different risk factors have different effects on the left versus the right CCA. However, the reason for these differences between left and right side CCA is not yet understood. It is assumed that it may be due to the different origins of the left and right CCA, whereby they are subjected to different flow intensities from the aortic arch. The left CCA stems directly from the arch of aorta and is affected by aortic arch pressure. The right CCA stems from the innominate artery, which is an extension of the ascending aorta, and is subjected to significant pressure from the ascending aortic blood flow. In addition, the wall shear stress resulting from the interaction between the blood and the intima has previously been associated with development of atherosclerotic plaque, a thick IMT, and vascular structural remodeling [38]. Reports in the literature [39] proposed that the IMT progression accelerates in the elderly and therefore could account for the difference in IMT seen at older ages that are non-existent in younger patients. Thus, we hypothesize that if mechanical shear stress forces do contribute to an accelerated development of the atherosclerotic process in the left carotid artery, they probably need a relatively prolonged period of time to become evident. Further studies are needed to elucidate this point of interest. Not only the IMT estimation, but also changes in the mechanical properties of the arterial wall are of interest as, they also have the potential

IEEE Journal of Translational Engineering in Health and Medicine

to signalize the existence of early cardiovascular disease. These changes can be detected by analyzing the arterial wall stiffness (or elasticity) using techniques such as diameter change estimation, artery distensibility or strain imaging [40]. In addition endarterectomies have a higher prevalence on the left side [29]. It was also suggested that increased shear forces in the left carotid artery contribute to this phenomenon.

There are also some limitations for the present study which arise mostly from the vascular dysfunction of the left and right CCA arteries which is affected by a number of factors [6], [9]. Furthermore, the presence of acoustic shadowing together with strong speckle noise hinders the visual and automatic analysis in ultrasound images. Poor quality images, with bad visual perception, were neither included in this study nor were they delineated by the experts [4]–[6], [22]. We have also excluded from our segmentation experiments images with extensive echolucency and calcification (40 and 10 from the normal group and CVD group corresponding to 4.1% and 8% of the number of images per group analyzed). Furthermore, the estimation and positioning of the initial snake contour may sometimes result to segmentation errors [41]. This should be placed as close as possible to the area of interest otherwise it may be trapped into local minima or false edges and converge to a wrong location. It should be noted that the parameters for each processing step (image normalization, despeckle filtering, the size of the moving pixel window, the number of iterations, IMC contour initialization, snakes segmentation) were selected for maximum performance. In the present study in less than 5% of the cases the positioning of the initial snake contour was not calculated correctly.

Future work will investigate the possible incorporation of the proposed IMC segmentation and IMT measurements tool into a computer aided diagnostic system that supports the texture analysis of the segmented IMC areas as well. More specifically, texture features [28], [31] and amplitude-modulation frequency-modulation multi-scale features [36] can be extracted from the IMC and used to discriminate between normal and CVD subjects.

REFERENCES

[1] S. Mendis, P. Puska, and B. Norrving, *Global Atlas on Cardiovascular Disease Prevention and Control*. Geneva, Switzerland: WHO, 2011.

[2] P. J. Touboul *et al.*, "Mannheim carotid intima-media thickness and plaque consensus (2004–2006–2011)," *Cerebrovascular Diseases*, vol. 34, no. 4, pp. 290–296, 2012.

[3] I. M. van der Meer, M. L. Bots, A. Hofman, A. I. del Sol, D. A. van der Kuip, and J. C. Witteman, "Predictive value of noninvasive measures of atherosclerosis for incident myocardial infarction: The Rotterdam Study," *Circulation*, vol. 109, no. 9, pp. 1089–1094, 2004.

[4] C. P. Loizou, "A review of ultrasound common carotid artery image and video segmentation techniques," *Med. Biol. Eng. Comput.*, vol. 52, no. 12, pp. 1073–1093, 2014.

[5] F. Molinari, G. Zeng, and J. S. Suri, "A state of the art review on intima–media thickness (IMT) measurement and wall segmentation techniques for carotid ultrasound," *Comput. Methods Programs Biomed.*, vol. 100, no. 3, pp. 201–221, 2010.

[6] Y. Arbel, N. Maharshak, A. Gal-Oz, I. Shapira, S. Berliner, and N. M. Bornstein, "Lack of difference in the intimal medial thickness between the left and right carotid arteries in the young," *Acta Neurol. Scandinavica*, vol. 115, no. 6, pp. 409–412, 2007.

[7] S. A. R. Hernandez *et al.*, "Is there a side predilection for cerebrovascular disease?" *Hypertension*, vol. 42, no. 1, pp. 56–60, 2003.

[8] Y. Sun, C.-H. Lin, C.-J. Lu, P.-K. Yip, and R.-C. Chen, "Carotid atherosclerosis, intima media thickness and risk factors—An analysis of 1781 asymptomatic subjects in Taiwan," *Atherosclerosis*, vol. 164, no. 1, pp. 89–94, 2002.

[9] X. Luo, Y. Yang, T. Cao, and Z. Li, "Differences in left and right carotid intima-media thickness and the associated risk factors," *Clin. Radiol.*, vol. 66, no. 5, pp. 393–398, 2011.

[10] S. W.-L. Lee *et al.*, "Side differences of carotid intima-media thickness in predicting cardiovascular events among patients with coronary artery disease," *Angiology*, vol. 62, no. 3, pp. 231–236, 2011.

[11] M. L. Bots, P. T. V. M. de Jong, A. Hofman, and D. E. Grobbee, "Left, right, near or far wall common carotid intima-media thickness measurements: Associations with cardiovascular disease and lower extremity arterial atherosclerosis," *J. Clin. Epidemiol.*, vol. 50, no. 7, pp. 801–807, 1997.

[12] C. Willekes, A. P. G. Hoeks, M. L. Bots, P. J. Brands, J. M. Willigers, and R. S. Reneman, "Evaluation of off-line automated intima–media thickness detection of the common carotid artery based on M-line signal processing," *Ultrasound Med. Biol.*, vol. 25, no. 1, pp. 57–64, 1999.

[13] J. M. Bland and D. G. Altman, "Statistical methods for assessing agreement between two methods of clinical measurement," *Lancet*, vol. 327, no. 8476, pp. 307–310, 1986.

[14] O. Onbas, M. Kantarci, A. Okur, U. Bayraktutan, A. Edis, and N. Ceviz, "Carotid intima-media thickness: Is it correlated with stroke side?" *Acta. Neurol. Scandinavica*, vol. 111, no. 3, pp. 169–171, 2005.

[15] C. Schmidt and I. Wendelhag, "How can the variability in ultrasound measurement of intima-media thickness be reduced? Studies of interobserver variability in carotid and femoral arteries," *Clin. Physiol.*, vol. 19, no. 1, pp. 45–55, 1999.

[16] C. P. Loizou, C. S. Pattichis, N. Georghiou, M. Griffin, and A. Nicolaides, "A comparison of ultrasound intima media thickness measurements of the left and right common carotid artery," in *Proc. IEEE 13th Int. Conf. Bioinformat. Bioeng. (BIBE)*, Chania, Greece, Nov. 2013, pp. 1–4, paper T.1.5.4.

[17] C. P. Loizou, C. S. Pattichis, M. Pantziaris, T. Tyllis, and A. Nicolaides, "Snakes based segmentation of the common carotid artery intima media," *Med. Biol. Eng. Comput.*, vol. 45, no. 1, pp. 35–49, 2007.

[18] C. P. Loizou, C. S. Pattichis, A. N. Nicolaides, and M. Pantziaris, "Manual and automated media and intima thickness measurements of the common carotid artery," *IEEE Trans. Ultrason., Ferroelectr., Freq. Control*, vol. 56, no. 5, pp. 983–994, May 2009.

[19] S. Petroudi, C. Loizou, M. Pantziaris, and C. Pattichis, "Segmentation of the common carotid intima-media complex in ultrasound images using active contours," *IEEE Trans. Biomed. Eng.*, vol. 59, no. 11, pp. 3060–3069, Nov. 2012.

[20] C. P. Loizou, C. S. Pattichis, C. I. Christodoulou, R. S. H. Istepanian, M. Pantziaris, and A. Nicolaides, "Comparative evaluation of despeckle filtering in ultrasound imaging of the carotid artery," *IEEE Trans. Ultrason., Ferroelectr., Freq. Control*, vol. 52, no. 10, pp. 1653–1669, Oct. 2005.

[21] "Comparison of image clarity, SonoCT real-time compound imaging versus conventional 2D ultrasound imaging," A Philips Med. Syst. Company, Tech. Rep., 2001.

[22] A. Nicolaides *et al.*, "The asymptomatic carotid stenosis and risk of stroke (ACSRS) study. Aims and results of quality control," *Int. Angiol.*, vol. 22, no. 3, pp. 263–272, 2003.

[23] T. Elatrozy, A. Nicolaides, T. Tegos, A. Z. Zarka, M. Griffin, and M. Sabetai, "The effect of B-mode ultrasonic image standardisation on the echodensity of symptomatic and asymptomatic carotid bifurcation plaques," *Int. Angiol.*, vol. 17, no. 3, pp. 179–186, 1998.

[24] J.-S. Lee, "Refined filtering of image noise using local statistics," *Comput. Graph. Image Process.*, vol. 15, no. 4, pp. 380–389, 1981.

[25] C. P. Loizou and C. S. Pattichis, "Despeckle filtering for ultrasound imaging and video, volume I: Algorithms and software," *Synthesis Lectures Algorithms Softw. Eng.*, vol. 7, no. 1, pp. 1–180, Apr. 2015.

[26] D. J. Williams and M. Shah, "A fast algorithm for active contours and curvature estimation," *CVGIP, Image Understand.*, vol. 55, no. 1, pp. 14–26, 1992.

[27] C.-C. Chang and C.-J. Lin, "LIBSVM: A library for support vector machines," *ACM Trans. Intell. Syst. Technol.*, vol. 2, no. 3, 2011, Art. ID 27. [Online]. Available: http://www.csie.ntu.edu.tw/~cjlin/libsvm

[28] E. C. Kyriacou *et al.*, "Prediction of high-risk asymptomatic carotid plaques based on ultrasonic image features," *IEEE Trans. Inf. Technol. Biomed.*, vol. 16, no. 5, pp. 966–973, Sep. 2012.
[29] B. G. Maxwell, J. G. Maxwell, and C. C. Brinker, "Left-side preference in carotid endarterectomies," *Amer. Surgeon*, vol. 66, no. 8, pp. 793–796, 2000.
[30] E. Vicenzini *et al.*, "Common carotid artery intima-media thickness determinants in a population study," *J. Ultrasound Med.*, vol. 26, no. 4, pp. 427–432, 2007.
[31] C. P. Loizou, M. Pantziaris, M. S. Pattichis, E. Kyriacou, and C. S. Pattichis, "Ultrasound image texture analysis of the intima and media layers of the common carotid artery and its correlation with age and gender," *Comput. Med. Imag. Graph.*, vol. 33, no. 4, pp. 317–324, 2009.
[32] S. Rosfors, S. Hallerstam, K. Jensen-Urstad, M. Zetterling, and C. Carlström, "Relationship between intima-media thickness in the common carotid artery and atherosclerosis in the carotid bifurcation," *Stroke*, vol. 29, no. 7, pp. 1378–1382, 1998.
[33] J. K. Balasundaram and R. S. D. W. Banu, "A non-invasive study of alterations of the carotid artery with age using ultrasound images," *Med. Biol. Eng. Comput.*, vol. 44, no. 9, pp. 767–772, 2006.
[34] S. Graf *et al.*, "Experimental and clinical validation of arterial diameter waveform and intimal media thickness obtained from B-mode ultrasound image processing," *Ultrasound Med. Biol.*, vol. 25, no. 9, pp. 1353–1363, 1999.
[35] M. Litwin *et al.*, "Altered morphologic properties of large arteries in children with chronic renal failure and after renal transplantation," *J. Amer. Soc. Nephrol.*, vol. 16, no. 5, pp. 1494–1500, 2005.
[36] C. P. Loizou, V. Murray, M. S. Pattichis, M. Pantziaris, and C. S. Pattichis, "Multiscale amplitude-modulation frequency-modulation (AM–FM) texture analysis of ultrasound images of the intima and media layers of the carotid artery," *IEEE Trans. Inf. Techol. Biomed.*, vol. 15, no. 2, pp. 178–188, Mar. 2011.
[37] C. P. Loizou, T. Kasparis, T. Lazarou, C. S. Pattichis, and M. Pantziaris, "Manual and automated intima-media thickness and diameter measurements of the common carotid artery in patients with renal failure disease," *Comput. Biol. Med.*, vol. 53, pp. 220–229, Oct. 2014.
[38] L. Lind, J. Andersson, A. Larsson, and B. Sandhagen, "Shear stress in the common carotid artery is related to both intima-media thickness and echogenecity: The prospective investigation of the vasculature in Uppsala seniors study," *Clin. Hemorheol. Microcirculat.*, vol. 43, no. 4, pp. 299–308, 2009.
[39] P. L. Allan, P. I. Mowbray, A. J. Lee, and F. G. R. Fowkes, "Relationship between carotid intima-media thickness and symptomatic and asymptomatic peripheral arterial disease. The Edinburgh Artery Study," *Stroke*, vol. 28, no. 2, pp. 348–353, 1997.
[40] M. Cinthio, A. R. Ahlgren, T. Jansson, A. Eriksson, H. W. Persson, and K. Lindstrom, "Evaluation of an ultrasonic echo-tracking method for measurements of arterial wall movements in two dimensions," *IEEE Trans. Ultrason., Ferroelectr., Freq. Control*, vol. 52, no. 8, pp. 1300–1311, Aug. 2005.
[41] S. Delsanto, F. Molinari, P. Giustetto, W. Liboni, S. Badalamenti, and J. S. Suri, "Characterization of a completely user-independent algorithm for carotid artery segmentation in 2-D ultrasound images," *IEEE Trans. Instrum. Meas.*, vol. 56, no. 4, pp. 1265–1274, Aug. 2007.

CHRISTOS P. LOIZOU, photograph and biography are not available at the time of publication.

ANDREW NICOLAIDES, photograph and biography are not available at the time of publication.

EFTHYVOULOS KYRIACOU, photograph and biography are not available at the time of publication.

NIKI GEORGHIOU, photograph and biography are not available at the time of publication.

MAURA GRIFFIN, photograph and biography are not available at the time of publication.

CONSTANTINOS S. PATTICHIS, photograph and biography are not available at the time of publication.